

27 May 2010, 4:30 pm - 6:20 pm

Cyclic Instability Behaviour of Sand-Silt Mixture Under Partial Cyclic Reversal Loading

Md. Abdul Lahil Baki

University of New South Wales at Australian Defense Force Academy, Australia

Sik-Cheung Robert Lo

University of New South Wales at Australian Defense Force Academy, Australia

Md. Mizanur Rahman

University of Canterbury, New Zealand

Follow this and additional works at: <https://scholarsmine.mst.edu/icrageesd>



Part of the [Geotechnical Engineering Commons](#)

Recommended Citation

Baki, Md. Abdul Lahil; Lo, Sik-Cheung Robert; and Rahman, Md. Mizanur, "Cyclic Instability Behaviour of Sand-Silt Mixture Under Partial Cyclic Reversal Loading" (2010). *International Conferences on Recent Advances in Geotechnical Earthquake Engineering and Soil Dynamics*. 11.

<https://scholarsmine.mst.edu/icrageesd/05icrageesd/session04/11>

This Article - Conference proceedings is brought to you for free and open access by Scholars' Mine. It has been accepted for inclusion in International Conferences on Recent Advances in Geotechnical Earthquake Engineering and Soil Dynamics by an authorized administrator of Scholars' Mine. This work is protected by U. S. Copyright Law. Unauthorized use including reproduction for redistribution requires the permission of the copyright holder. For more information, please contact scholarsmine@mst.edu.



Fifth International Conference on

Recent Advances in Geotechnical Earthquake Engineering and Soil Dynamics and Symposium in Honor of Professor I.M. Idriss

May 24-29, 2010 • San Diego, California

CYCLIC INSTABILITY BEHAVIOUR OF SAND-SILT MIXTURE UNDER PARTIAL CYCLIC REVERSAL LOADING

Md. Abdul Lahil Baki

University of New South Wales at
Australian Defence Force Academy,
Canberra, ACT, Australia 2600

Sik-Cheung Robert Lo

University of New South Wales at
Australian Defence Force Academy,
Canberra, ACT, Australia 2600

Md. Mizanur Rahman

University of Canterbury, Christchurch,
New Zealand 8140

ABSTRACT

Flow liquefaction is one of the most catastrophic failure phenomena in geotechnical engineering. It is a form of instability and can be observed during monotonic loading or cyclic loading. It is referred to as static instability/liquefaction for monotonic loading and cyclic instability for cyclic loading. To investigate the link between these behaviours, a number of stress controlled cyclic triaxial tests were carried out on loose sand-silt mixture under cyclic 'reversal' and 'non-reversal' loading condition. Cyclic reversal loading was partial reversal. Its peak-trough magnitudes were chosen in such a way that cyclic instability was triggered in compression side of the stress space. Thus it gives an opportunity to compare cyclic instability (both for partial 'reversal' and 'non-reversal') with static instability observed in monotonic loading condition. The test condition covers a range of initial mean effective confining stresses and void ratio. The equivalent granular state parameter was used to synthesize the test results irrespective of fines contents.

Test results showed that cyclic instability was governed by the stress ratio at static instability for the same equivalent granular state parameter irrespective of fines contents. Thus, equivalent granular state parameter can be used as a predictor of cyclic instability for cyclic 'reversal' and 'non-reversal' loading if cyclic instability is triggered in compression side of the stress space.

INTRODUCTION

Liquefaction related failures due to earthquake are the most devastating failure noticed from last few decades. Cohesionless soils like clean sand as well as sand-silt mixture are the most susceptible for liquefaction (Athanasopoulos and Xenaki 2008; Bobei et al. 2009; Cubrinovski and Rees 2008; Murthy et al. 2007; Thevanayagam and Ecemis 2008). Loose sand or sand-silt mixture under undrained shearing can manifest instability under either monotonic or cyclic loading. An important concept in the interpretation of instability is the instability line, IL (Chu and Leong 2002; Lo et al. 2008b; Yang 2002).

Sladen et al. (1985) introduced the collapse line, CL as a straight line joining peak points of undrained effective stress

path, ESP (normalized by mean effective stress at steady state, SS) and the corresponding steady state, SS points for same void ratio to predict initiation of instability. On the other hand, Lade (1993) introduced instability line, IL that joining peak points of undrained effective stress path, ESP for same void ratio and it passes through the origin of stress space. A number of researchers reported a similar finding (Chu and Wanatowski 2008; Lo et al. 2008b; Yang et al. 2006). As instability line passes through the origin of the stress space, the slope of the IL is the stress ratio at onset of instability and it is denoted as η_{IS} . However, within this paper the onset instability is referred to the stress ratio, η_{IS} at instability instead of a line as it encapsulates the concept of IL but avoid the geometric presentation of IL.

Many researchers emphasised to link between monotonic and cyclic behaviour under triaxial test (Gennaro et al. 2004; Hyodo et al. 1994; Lo et al. 2008a; Mohamad and Dobry 1986; Vaid and Sivathayalan 2000; Yamamuro and Covert 2001). Of them, Yamamuro and Covert (2001) demonstrated that instability line derived from the undrained monotonic tests also defined the trigger line for cyclic liquefaction for Nevada sand contained 40% silt. Gennaro et al. (2004) also demonstrated that for a given initial density, the undrained monotonic behaviour can help to predict the behaviour during undrained cyclic loading. However, Alarcon-Guzman et al. (1988) based on torsional shear test result on Ottawa sand showed that for a given void ratio, monotonic ESP determines the initiation of strain softening behaviour under cyclic loading. Hyodo et al. (1994) demonstrated that cyclic instability was triggered when cyclic ESP reached the instability region of corresponding monotonic test.

Chu and Wanatowski (2008) unambiguously demonstrated that the slope of an instability line is dependent on void ratio and it poses a correlation in $\eta_{IS}-e$ space. This undermines the effectiveness of the instability stress ratio as a means for predicting onset of instability as one can infer it from the correlation in $\eta_{IS}-e$ space. However, Yang (2002) claimed a better correlation can be achieved for a large number of data sets in $\eta_{IS}-\psi$ space, where ψ is the state parameter as defined by Been and Jefferies (1985). However, for sand with fines, there is an additional complication that void ratio, e is not an effective parameter to capture the effect of fines in soil behaviour. The equivalent granular void ratio, e^* and equivalent granular state parameter, ψ^* (discussed later) are believed to be an appropriate parameter for sand with fines (Chiu and Fu 2008; Rahman and Lo 2007a). The objective of this paper is to evaluate the correspondence between monotonic and cyclic instability behaviour and to verify whether one can identify cyclic instability for a cyclic test from its state i.e. ψ^* using a pre-established instability relationship in $\eta_{IS}-\psi^*$ space from monotonic tests.

BACKGROUND ON MODELLING EFFECTS OF FINES

Equivalent Granular Void Ratio

The recent achievements in modelling the influence of fines in sand are discussed in this section. The discussion is limited to “fines-in-sand” soil fabric, i.e. when the fines content is less than a threshold value referred to as threshold fines content, f_{thre} . In this case, fines are mainly located between the void spaces formed by coarse particles and may or may not be taking an effective role in the force structure. To capture such a feature, the equivalent granular void ratio, e^* was introduced by Thevanayagam et al. (2002) as:

$$e^* = \{e + (1-b)f_c\} / \{1 - (1-b)f_c\} \quad (1)$$

where b represents the fraction of fines that actively take part in the force structure of mixed sand and therefore $1 \geq b \geq 0$. As discussed in Rahman et al. (2009), b has to be an increasing function of f_c to be consistent with binary packing. Most of the reported b values (Chiu and Fu 2008; Ni et al. 2004; Yang et al. 2006) were back-analysed values on the assumption that a single correlation exist for sand with fines behaviour at SS or cyclic resistance (CR) to liquefaction. Thus, large number of data for sand with fines are required for back analysis and this was the major difficulty in conversion e^* from e . To overcome this challenge, Rahman et al. (2008; 2009) developed a model to determine b from simple input parameter such as diameter ratio and fines content.

$$b = \left[1 - \exp\left(-0.3 \frac{(f_c / f_{thre})}{k}\right) \right] \times \left(r \frac{f_c}{f_{thre}} \right)^r \quad (2)$$

where $r = (D_{10}/d_{50})^{-1} = d_{50}/D_{10}$, $k = (1 - r^{0.25})$. D_{10} = size of sand at 10% finer and d_{50} = size of fines at 50% finer. e^* can be calculated using Eqns. 1 and 2; will give a single correlation between e^* and CR, and a narrow trend line between e^* and SS points in $e^*-\log(p')$ space was clearly demonstrated by (Rahman and Lo 2007b; Rahman and Lo 2008b; Rahman et al. 2008; Rahman et al. 2009). The narrow trend line in $e^*-\log(p')$ space can be approximated an alternative steady state line, SSL for sand with fines and it is referred to as equivalent granular Steady State Line, EG-SSL by Rahman et al. (2009). A more detail version of this literature can be found in another paper submitted to this conference (Rahman et al. 2010).

Equivalent Granular State Parameter

The state parameter, ψ as defined by Been and Jefferies (1985) is generally a good parameter than void ratio for predicting the instability behaviour of a sandy soil. In general, when $\psi > 0$ one can expect instable behaviour and thus, Yang (2002) reported correlation between ψ and η_{IS} in $\psi-\eta_{IS}$ space. Considering the complexity of sand-fines behaviour, Rahman and Lo (2007a) introduced equivalent granular state parameter in line with state parameter (Been and Jefferies 1985) as shown in Fig. 1. The equivalent granular state parameter can be presented as:

$$\psi^* = e^* - e^*_{SS} \quad (3)$$

where e^*_{SS} is the equivalent granular void ratio at SS. Similar approach can be found in (Chiu and Fu 2008; Thevanayagam et al. 2002). To denote equivalent granular state parameter at the start of undrained shearing; the symbol $\psi^*(0)$ will be used hereafter.

Hypothesis

It is hypothesized in this paper that there is a correspondence between static and cyclic instability i.e. cyclic instability

triggered at near about same instability stress ratio as in monotonic test with a initial condition same as the cyclic test. Thus, the relation between $\psi^*(0)$ and η_{IS} for monotonic loading condition in $\psi^*(0)$ - η_{IS} space can be used as a predictor for onset cyclic instability for a known initial state i.e. $\psi^*(0)$ and this should be equally applicable irrespective of fines contents.

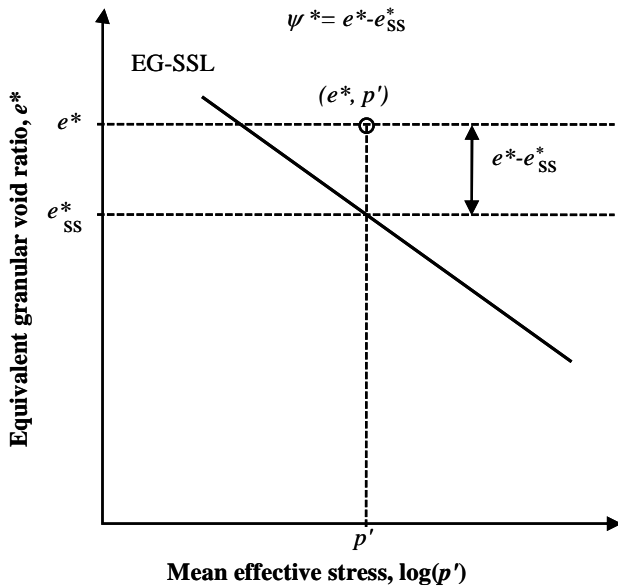


Fig. 1. Definition of ψ^* (after Rahman and Lo, 2007)

EXPERIMENTAL PROGRAMME

Testing System

Testing program was designed in such a way that a wide range of effective initial confining stress, p_0' (350-1300 kPa) was covered. A fully automated data logging facilities was used for data recording and an in-house built programme was used to control the loading frame. The axial deformation was measured by two internal linear variable differential transformers (LVDT) attached on the top platen. An external LVDT was also used to measure the axial deformation when internal LVDTs went out of the limit. Cell pressure and pore pressure was controlled and measured by large and small Digital Pressure Volume Controllers (DPVC) respectively. Pore pressure equilibrium also checked using two pressure transducers. An internal load cell was used to record the axial load without friction and an external load cell was used to achieve load control condition. The difference between internal and external load cell reading due to friction was calibrated so that applied force on the top of the specimen can be controlled. To apply loading in extension side, the loading ram was screwed onto the top platen under p_0' of 70 kPa. The effective mean confining stress was then ramped gradually to the desired initial value. To achieve isotropic loading, the external load was adjusted so that deviator stress $q \approx 0$ in

internal load cell. After reaching the desired consolidation pressure, the sample was kept consolidation stage for 10-12 hours to ensure proper consolidation. Then a cyclic sinusoidal force was applied in a frequency of 1800 sec/cycle with different peak and trough value.

Material Tested

Clean uniform size quartz sand (SP) called Sydney sand was used as host sand. Well-graded fines was used in all tests by mixing 2/3 Majura fines and 1/3 commercially available kaolin. Majura fines was collected from Majura river bank deposit. Figure 2 shows the grain size distribution curve of the tested materials and the physical properties can be found in Rahman and Lo (2008a). Fines used in this study ranged between 15-30% by dry weight.

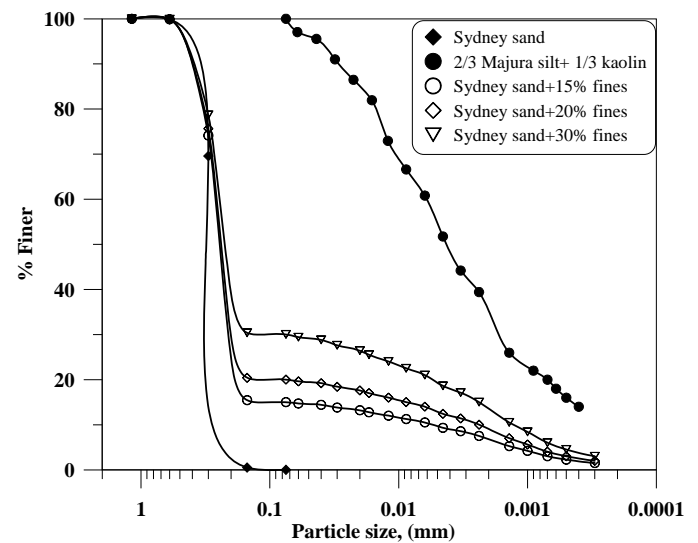


Fig. 2. Grading curves

Specimen Preparation

Cylindrical specimens of 100 mm height and 100 mm diameter were prepared by placing and lightly tamping predetermined quantity of material (of known moisture content) to a 10 mm thick layer. Free ends with enlarged platens were used to reduce end restraint to an insignificant level as discussed in Lo et al. (1989). Liquid rubber technique was also used to effectively reduce bedding and membrane penetration errors (Lo et al. 1989). After preparing the sample, a small vacuum pressure of 20 kPa was applied to remove entrapped air from the sample. Then, a small water head of 1 m was used to flash the sample under the vacuum pressure. Finally saturation was ensured by back-pressure technique with Skempton's B-value of 0.98 or more in each case.

Accurate measurement of void ratio is essential to the interpretation of test results within CSSM framework. The

dimensions of the specimen could be measured accurately at the end of vacuum flushing. However, during back pressure saturation, only axial strain change, $\delta\varepsilon_1$, can be measured by the internal LVDT. Change in volume strain had to be inferred from the relation $\delta\varepsilon_v \approx 3\delta\varepsilon_1$, noting the effective stress change during saturation is isotropic. This approximation is acceptable as $\delta\varepsilon_1$ was small. This enabled the determination of void ratio at the end of consolidation.

RESULT AND ANALYSIS

Monotonic and Cyclic Tests

A series of undrained monotonic tests were conducted on sandy soil covering a range of fines contents, $f_c = 0-30\%$ and $p_0' = 350-1300$ kPa at different void ratio prior to the shearing. The details of the testing can be found in Rahman (2009). The η_{IS} obtained for those monotonic tests were plotted with their corresponding $\psi^*(0)$ in $\psi(0)-\eta_{IS}$ space as shown in Fig. 3. This correlation formed a single trend line irrespective of f_c and p_0' . It is pertinent to note that sometime it is difficult or unreasonable to pick a single point for η_{IS} from each test due to absence of sharp peak deviator stress on undrained monotonic ESP. Thus, each point in the figure shows a bar for possible variation.

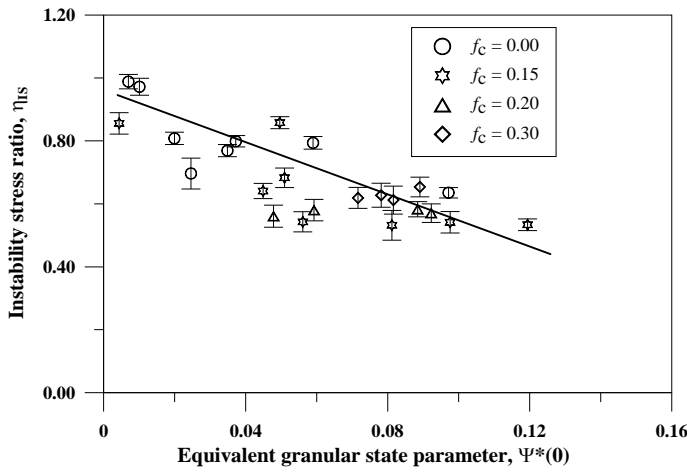


Fig. 3. Relation between instability stress ratio, η_{IS} and the equivalent granular state parameter, $\psi^*(0)$

A series of undrained cyclic triaxial tests were conducted on sandy soil, covering fines contents, $f_c = 15\%-30\%$ and $p_0' = 350-850$ kPa at different void ratio prior to the shearing. The details of the testing can be found in Table 1 but only few of them are discussed in details within the scope of this conference paper. Cyclic testing programme was covered both cyclic 'non-reversal' and partial 'reversal' loading. In case of cyclic 'non-reversal' loading, peak and trough magnitude was controlled by the external load cell in such a way that cyclic deviator stress, q varied within the positive side in $p'-q$ space. For cyclic partial 'reversal' loading, the trough was in

extension side and its magnitude was less than 50% of that in compression side (peak), so that any potential instability was occurred in compression side of $p'-q$ space.

Table 1. Summary of Tests Results

Test Name	Test Type	Fines (%)	p_0' (kPa)	e^*	$\psi^*(0)$
M-20-14	Monotonic	20	600	0.874	+0.059
C-20-39	Cyclic Non-reversal	20	600	0.868	+0.053
C-15-41	Cyclic Non-reversal	15	600	0.853	+0.038
C-15-79	Cyclic Part. Reversal	15	600	0.919	+0.104
C-15-87	Cyclic Part. Reversal	15	600	0.928	+0.114
C-15-92	Cyclic Part. Reversal	15	600	0.905	+0.091
C-20-66	Cyclic Non-reversal	20	850	0.845	+0.056
C-20-65	Cyclic Part. Reversal	20	350	0.902	+0.058
C-20-68	Cyclic Part. Reversal	20	850	0.879	+0.090
C-30-61	Cyclic Part. Reversal	30	350	0.895	+0.052
C-30-80	Cyclic Part. Reversal	30	600	0.875	+0.061

Relationship between Monotonic and Cyclic Instability

The aim of this section is to demonstrate the correspondence of between monotonic and cyclic instability behaviour. One monotonic (M-20-14) and one cyclic test (C-20-39) for sand with 20% fines content are presented in Fig. 4(a-b). The tests, M-20-14 and C-20-39 are sheared from nearly same initial condition and their corresponding $\psi^*(0)$ are +0.059 and +0.053 respectively. Static instability behaviour was observed for M-20-14 at a peak deviator stress ratio, $\eta_{IS}=0.580$. After that flow type behaviour was observed with large axial strain as shown by dotted line in Fig. 4(a-b). A solid line with $\eta_{IS}=0.580$ was drawn through the peak q of monotonic ESP but due to the flat peak one may find a narrow range in η_{IS} around $\eta_{IS}=0.580$. Next, to observe the cyclic instability behaviour, a replicate sample, C-20-39 was prepared with a nearly same $\psi^*(0)$ of +0.053. Test C-20-39 was sheared with a peak deviator stress of 195 kPa in first 15 cycles but the movement of ESP in $p'-q$ space was very slow and there was no sign of cyclic instability. It is pertinent to note that though the ESP at the beginning was problematic but did not affect on later stage to develop pore water pressure (pwp). Thereafter, a second cyclic stress pulse with a peak deviator stress of 255 kPa was applied and after 4th cycle sample showed cyclic

instability with large axial strain as shown in Fig. 4(a-b). In this case, it was also difficult to find precise triggering point of cyclic instability because only one peak value was available for corresponding six cycles and ESP shifted left side due to pwp generation in consecutive next cycles. However, the movement of ESP to the left increased after 4th cycle and can be consider as trigger points which is very close to $\eta_{IS}=0.580$ for corresponding monotonic loading. Thus, a good correspondence was observed between monotonic and cyclic instability behaviour and the triggering mechanism was controlled by η_{IS} obtained from monotonic test. The above observations also in line with (Lo et al. 2008b) and many others (Hyodo et al. 1994; Yamamuro and Covert 2001).

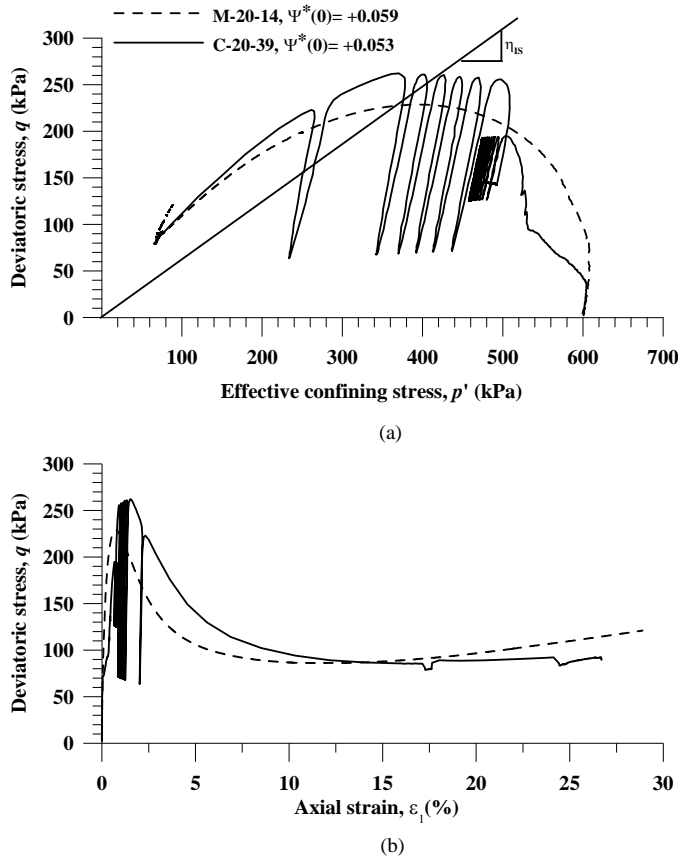


Fig. 4. Test pair M-20-14 and C-20-39 with $\psi^*(0) = +0.059$ and $+0.053$ respectively for 20% fines (a) ESP and (b) q - ϵ_1 plot

Prediction of Cyclic Instability from Monotonic ψ - η_{IS} Relation

The relation between $\psi^*(0)$ and η_{IS} in the $\psi(0)$ - η_{IS} space can be obtained from monotonic tests irrespective of fines contents as shown in Fig. 3. This relation was used in this paper to predict probable cyclic instability behaviour by the following steps:

- Calculate void ratio prior to the shearing and convert it to e^* using Eqns.2 and 1.

- Calculate $\psi^*(0)$ using Eqn. 3.
- Pick up η_{IS} for the corresponding $\psi^*(0)$ from Fig. 3 and this is the probable triggering instability for cyclic loading.

Prediction of Cyclic Instability for 15% Fines (Cyclic Non-reversal Loading)

The ESP and q - ϵ_1 plot for one way cyclic loading test (C-15-41) is shown in Fig. 5(a-b) conducted on sand with 15% fines content at an initial effective confining pressure of 600 kPa.

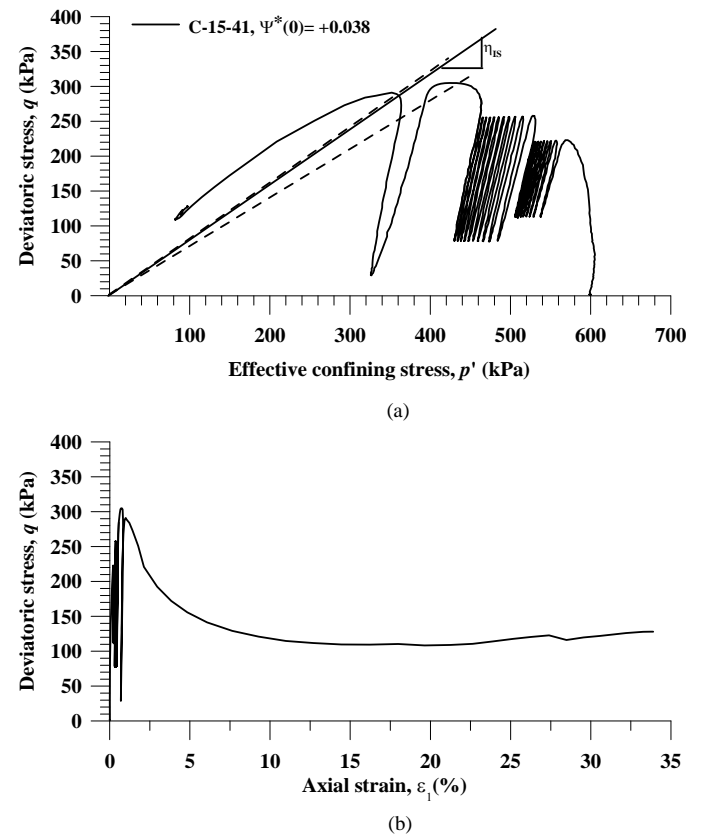


Fig. 5. Relationship between monotonic and cyclic instability with $\psi^*(0) = +0.038$ for 15% fines (a) ESP and (b) q - ϵ_1 plot

The initial void ratio was 0.853 and the corresponding $\psi^*(0)$ values was $+0.038$. First the specimen sheared with a packet of stress pulse had a peak deviator stress, q_{peak} of 222 kPa. Therefore cyclic ESP was moved left side at a slow rate in consecutive 8 cycles without any noticeable cyclic instability. Then a second packet of stress pulse was applied with higher q_{peak} of 255 kPa. Though the movement of cyclic ESP was faster than first packet of stress pulse, still no sign of cyclic instability was noticed. Therefore, a third packet stress pulse with q_{peak} of 305 kPa was applied and instability was triggered. To predict the cyclic instability (or stress ratio at cyclic instability) for this test the η_{IS} corresponding to the $\psi^*(0) = +0.038$ was read from Fig. 3 (which is obtained from monotonic loading) shown by the solid line in Fig. 5(a). The

range of η_{IS} (0.693-0.812) where cyclic instability was expected was plotted by two dotted lines in Fig. 5(a). After triggering the cyclic instability, soil sample manifested large axial strain as shown in Fig. 5(b). It is pertinent to note that cyclic ESP had no sharp peak cyclic instability stress ratio during onset of cyclic instability rather ranged in between 0.693 to 0.812. Thus stress ratio at cyclic instability can be predicted from monotonic η_{IS} for sand with fines when test results synthesize with $\psi^*(0)$.

Prediction of Cyclic Instability for 20% Fines (Cyclic Non-reversal Loading)

The ESP and q - ε_1 response for sand with 20% fines content are presented in Fig. 6(a) and Fig. 6(b) respectively. This is also a one way cyclic loading test. Test was conducted at an initial effective confining pressure of 850 kPa with initial void ratio 0.845 and $\psi^*(0) = +0.056$. The sample was first sheared by applying monotonic load to a deviator stress of 303 kPa, and then first packet of cyclic load was applied with a q_{peak} of 303 kPa. In first 15 cycles, cyclic effective stress ratio remained below the η_{IS} and stress path moved slowly leftward without any sign of cyclic instability. Therefore a second packet of cyclic loading with bit higher q_{peak} of 314 kPa was applied. Cyclic instability was manifested at 4th cycle when second packet of stress pulse was just crossing the η_{IS} (presented by dotted line). In this case, the η_{IS} corresponding to the $\psi^*(0) = 0.056$ was also read from Fig. 3 to predict cyclic instability (or stress ratio at cyclic instability). Stress ratio at cyclic instability was close to η_{IS} (obtained from monotonic test) and it was a narrow band (0.708-0.738) around η_{IS} shown by two dotted lines in 6(a).

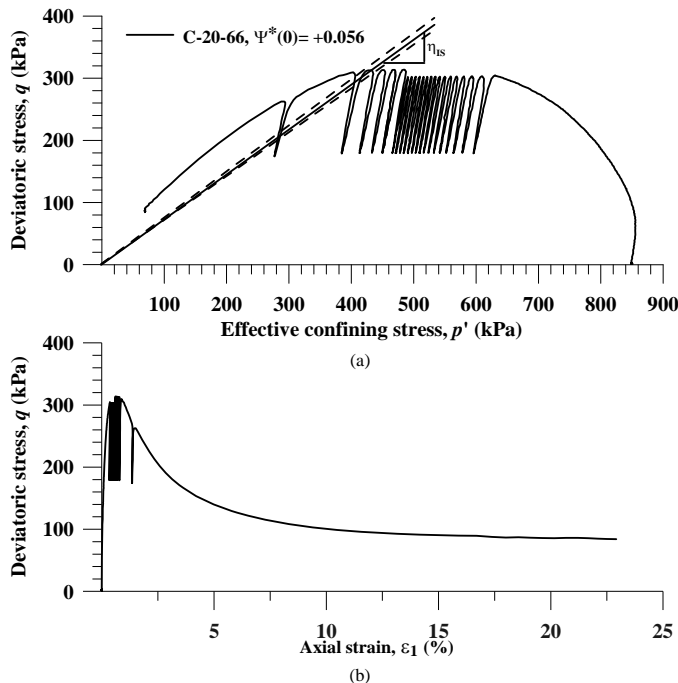


Fig. 6. Relationship between monotonic and cyclic instability with $\psi^*(0) = +0.056$ for 20% fines (a) ESP and (b) q - ε_1 plot

Hence, it can be concluded that η_{IS} obtained from monotonic test was the predictor of onset of cyclic instability for cyclic non-reversal loading.

Prediction of Cyclic Instability for 30% Fines (Cyclic Partial Reversal Loading)

A partial cyclic reversal loading test was conducted on sand with 30% fines content at an initial effective confining pressure of 350 kPa. The initial void ratio was 0.895 and the corresponding $\psi^*(0)$ values was +0.052. ESP and q - ε_1 plot is presented by Fig. 7(a-b) whereas Fig. 7(c) shows pwp- ε_1 response.

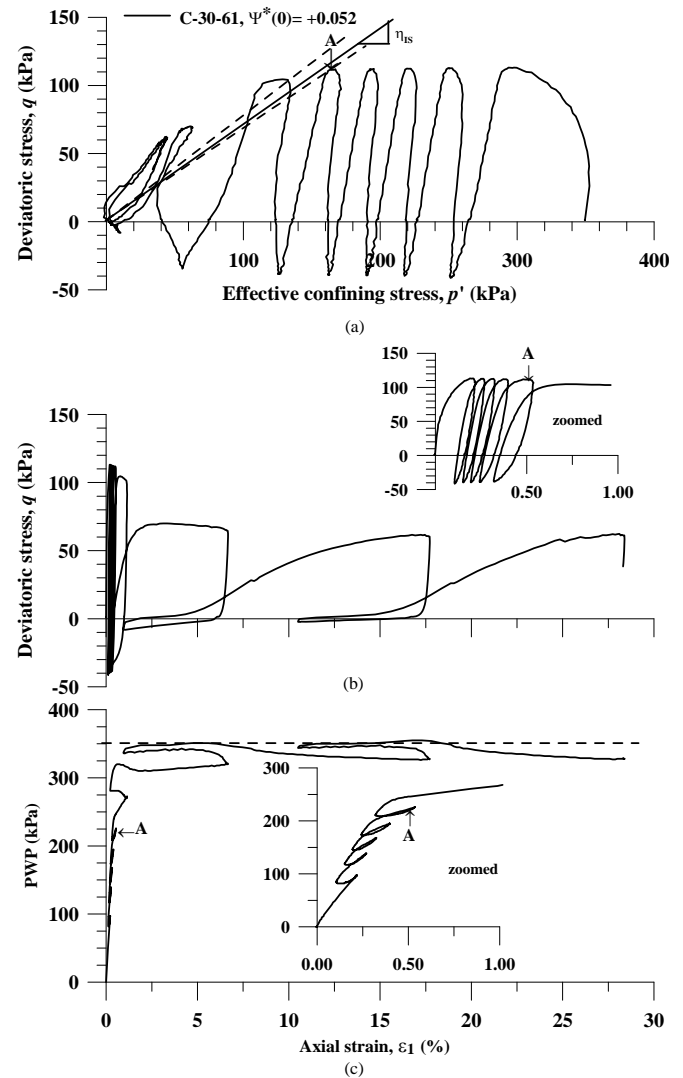


Fig. 7. Relationship between monotonic and cyclic instability with $\psi^*(0) = +0.052$ for 30% fines (a) ESP, (b) q - ε_1 , (c) pwp- ε_1 plot

Cyclic ESP had a q_{peak} of 112 kPa and q_{min} of -39kPa in compression and extension side of stress space respectively. It is pertinent to restate that a smaller deviator stress was applied in the extension side so that any potential instability was

triggered on the compression side in $p'-q$ stress space. Cyclic ESP was moved left side of stress space steadily up to 4th cycle with peak cyclic stress pulse less η_{IS} . The pwp was higher in the first cycle and the cyclic ESP moved steadily in next 4 cycles until crossed the point "A" as indicated in Fig. 7(a). Pwp and axial strain was started to increase dramatically after that point. The range of η_{IS} where cyclic instability was expected was plotted by two dotted lines in Fig. 7(a). In the same figure, a solid line shows the η_{IS} line corresponding to the $\psi^*(0) = 0.052$ that was read from Fig. 3. It was observed that cyclic instability was triggered after point 'A' with the development of large axial strain and the η_{IS} value was within the expected range (0.700-0.780) as marked by dotted line. Hence it can be concluded that the η_{IS} obtained from monotonic test was the triggering point for onset of cyclic instability for tested material under partial cyclic reversal loading condition.

CONCLUSION

A series of cyclic triaxial tests were conducted to investigate the link between static and cyclic instability behaviour. An attempt has been made to predict cyclic instability behaviour for an initial condition from pre-established relation from monotonic test. The test condition was covered wide range of fines (15-30%), ψ^* , cyclic loading (non-reversal and partial reversal). Based on this experimental study, the following concluding remarks are summarised.

- There is a link between Cyclic and Monotonic Instability.
- Monotonic instability possesses a relation in $\eta_{IS}-\psi^*(0)$ space irrespective of fines contents.
- The $\eta_{IS}-\psi^*(0)$ relation obtained from monotonic tests can be used to predict cyclic instability irrespective of fines contents.

The above findings are limited to $\psi^*(0) > 0$ and the instability occurs in compression side of stress space. The concept of equivalent granular void ratio and equivalent state parameter is limited to gap graded sand and round shaped particles mentioned in Rahman et al. (2008).

ACKNOWLEDGEMENTS

The first author is currently supported by the University College Postgraduate Research Scholarship (UCPRS) and conducting his research at UNSW@ADFA. The first and third author would like to acknowledge the support (study leave) from the Rajshahi University of Engineering & Technology (RUET), Bangladesh.

REFERENCE

- Alarcon-Guzman, A., Leonards, G. A., and Chameau, J. L. [1988]. "Undrained Monotonic and Cyclic Strength of Sand." *Journal of Geo. Engrg.*, Vol., 114, No. 10, pp. 1089-1109.
- Athanasopoulos, G. A., and Xenaki, V. C. [2008]. "Liquefaction resistance of sands containing varying amounts of fines." *4th decennial Geo. Erthq. Engrg. and Soil Dyn. Conf.*, GSP-181, ASCE, Sacramento, California, USA.
- Been, K., and Jefferies, M. G. [1985]. "A State Parameter for Sands." *Géotechnique*, Vol., 35, No. 2, pp. 99-112.
- Bobei, D. C., Lo, S. R., Wanatowski, D., Gnanendran, C. T., and Rahman, M. M. [2009]. "A Modified State Parameter for Characterizing Static Liquefaction of Sand with Fines." *Can. Geo. Journal*, Vol., 46, No. 3, pp. 281-295.
- Chiu, C. F., and Fu, X. J. [2008]. "Interpreting Undrained Instability of Mixed Soils by Equivalent Intergranular State Parameter." *Geotechnique*, Vol., 58, No. 9, pp. 751-755.
- Chu, J., and Leong, W. K. [2002]. "Effect of Fines on Instability Behaviour of Loose Sand." *Geotechnique* Vol., 52, No. 10, pp. 751-755.
- Chu, J., and Wanatowski, D. [2008]. "Instability Conditions of Loose Sand in Plane Strain." *Journal of Geo. and Geoenviron. Engrg.* Vol., 134, No.1, pp. 136-142.
- Cubrinovski, M., and Rees, S. [2008]. "Effects of Fines on Undrained Behaviour of Sands." *4th decennial Geo. Erthq. Engrg. and Soil Dyn. Conf.*, GSP-181, ASCE, Sacramento, California, USA.
- Gennaro, V. D., Canou, J., Dupla, J. C., and Benahmed, N. [2004]. "Influence of Loading Path on the Undrained Behaviour of a Medium Loose Sand." *Can. Geo. Journal*, Vol., 41, No. 1, pp. 166.
- Hyodo, M., Tanimizu, H., Yasufuku, N., and Murata, H. [1994]. "Undrained Cyclic and Monotonic Triaxial Behaviour of Saturated Loose Sand." *Soils and Found.*, Vol., 34, No. 1, pp. 19-32.
- Lade, P. V. [1993]. "Initiation of Static Instability in the Submarine Nerlerk Berm." *Can. Geo. Journal*, Vol., 30, pp. 895-904.
- Lo, S. R., Chu, J., and Lee, I. K. [1989]. "A Technique for Reducing Membrane Penetration and Bedding Errors." *Geo. Testing Journal*, Vol., 12, No. 4, pp. 311-316.
- Lo, S. R., Rahman, M. M., and Bobei, D. [2008a]. "Limited Flow Behaviour of Sand with Fines under Monotonic and Cyclic Loading." *Proc. of the 2nd Intern. Conf. on Geo. Engrg for Disaster Mitigation & Rehab. (GEDMAR08)*, Nanjing, China, pp. 201-209.

- Lo, S. R., Rahman, M. M., and Bobei, D. C. [2008b]. "Limited Flow Behaviour of Sand with Fines under Monotonic and Cyclic Loading." *Geomec. and Geoengr.*, In Print.
- Mohamad, R., and Dobry, R. [1986]. "Undrained Monotonic and Cyclic Triaxial Strength of Sand." *Journal of Geo. Engrg.*, Vol. 112, No.10, pp. 941-958.
- Murthy, T. G., Loukidis, D., Carraro, J. A. H., Prezzi, M., and Salgado, R. [2007]. "Undrained Monotonic Response of Clean and Silty Sands." *Geotechnique*, Vol. 57, No. 3, pp. 273-288.
- Ni, Q., Tan, T. S., Dasari, G. R., and Hight, D. W. [2004]. "Contribution of Fines to the Compressive Strength of Mixed Soils." *Geotechnique*, Vol., 54, No. 9, pp. 561-569.
- Rahman, M. M. [2009]. "*Modelling the Influence of Fines on Liquefaction Behaviour*," PhD Thesis, University of New South Wales at Australian Defence Force Academy, Canberra, Australia.
- Rahman, M. M., and Lo, S. C. R. [2007a]. "Equivalent Granular Void Ratio and State Parameters for Loose Clean Sand with Small Amount of Fines." *Common Ground Proc. 10th Aus. New Zealand Conf. on Geomechanics*, Brisbane, Australia, pp. 674-679.
- Rahman, M. M., and Lo, S. R. [2007b]. "On Intergranular void ratio of loose sand with small amount of fines." *16th South East Asian Geo. Conf.*, Kuala Lumpur, Malaysia, pp. 255-260.
- Rahman, M. M., and Lo, S. R. [2008a]. "Effect of Sand Gradation and Fines Type on Liquefaction Behaviour of Sand-fines Mixture." *4th decennial Geo. Erthq. Engrg. and Soil Dyn. Conf.*, GSP-181, ASCE, Sacramento, California, USA.
- Rahman, M. M., and Lo, S. R. [2008b]. "The Prediction of Equivalent Granular Steady State Line of Loose Sand with Fines." *Geomec. and Geoengr.*, Vol., 3, No. 3, pp. 179--190.
- Rahman, M. M., Lo, S. R., and Cubrinovski, M. [2010]. "Equivalent granular void ratio and behaviour of loose sand with fines." *5th Intern. Conf. on recent Adv. in Geo. Erthq. Engrg. and Soil Dyn.*, San Diego, California, Submitted to this conference.
- Rahman, M. M., Lo, S. R., and Gnanendran, C. T. [2008]. "On Equivalent Granular Void Ratio and Steady State Behaviour of Loose Sand with Fines." *Can. Geo. Journal*, Vol., 45, No. 10, pp. 1439-1456.
- Rahman, M. M., Lo, S. R., and Gnanendran, C. T. [2009]. "Reply to discussion by Wanatowski, D. and Chu, J. on- On Equivalent Granular Void Ratio and Steady State Behaviour of Loose Sand with Fines." *Can. Geo. Journal*, Vol., 46, No. 4, pp. 483-486.
- Sladen, J. A., D'Hollander, R. D., and Krahn, J. [1985]. "The Liquefaction of sands, a Collapse Surface Approach." *Can. Geo. Journal*, Vol., 22, No. 4, pp. 564-578.
- Thevanayagam, S., and Ecmis, N. [2008]. "Effects of Permeability on Liquefaction Resistance and Cone Resistance." *4th decennial Geo. Erthq. Engrg. and Soil Dyn. Conf.*, GSP-181, ASCE, Sacramento, California, USA.
- Thevanayagam, S., Shenthan, T., Mohan, S., and Liang, J. [2002]. "Undrained Fragility of Clean Sands, Silty Sands, and Sandy Silts." *Journal of Geo. and Geoenviron. Engrg.*, Vol., 128, No. 10, pp. 849-859.
- Vaid, Y. P., and Sivathayalan, S. [2000]. "Fundamental Factors Affecting Liquefaction Susceptibility of Sands." *Can. Geo. Journal*, Vol., 37, No. 3, pp. 592-606.
- Yamamuro, J. A., and Covert, K. M. [2001]. "Monotonic and Cyclic Liquefaction of Very Loose Sands with High Silt Content." *Journal of Geo. and Geoenviron. Engrg.*, Vol., 127, No. 4, pp. 314-324.
- Yang, J. [2002]. "Non-uniqueness of Flow Liquefaction Line for Loose Sand." *Geotechnique*, Vol., 52, No. 10, pp. 757-760.
- Yang, S. L., Sandven, R., and Grande, L. [2006]. "Instability of Sand-silt Mixtures." *Soil Dyn. and Erthq. Engrg.*, Vol., 26, No. 2-4, pp. 183-190.